

## Ac Losses in Superconducting Parallel Conductors in Saturation Case

**Tanaka, Hideki**

Department of Electrical and Electronic Systems Engineering, Graduate School of Information Science and Electrical Engineering, Kyushu University : Graduate Student

**Iwakuma, Masataka**

Department of Electrical and Electronic Systems Engineering, Faculty of Information Science and Electrical Engineering, Kyushu University

**Funaki, Kazuo**

Department of Electrical and Electronic Systems Engineering, Faculty of Information Science and Electrical Engineering, Kyushu University

<https://doi.org/10.15017/1525437>

---

出版情報 : 九州大学大学院システム情報科学紀要. 7 (1), pp.13-18, 2002-03-26. 九州大学大学院システム情報科学研究所

バージョン :

権利関係 :

## Ac Losses in Superconducting Parallel Conductors in Saturation Case

Hideki TANAKA\* , Masataka IWAKUMA\*\* and Kazuo FUNAKI\*\*

(Received December 14, 2001)

**Abstract:** Ac loss properties of 2-strand superconducting parallel conductors in the saturation case are quantitatively discussed. The parallel conductors are composed of rectangular cross-sectional multifilamentary strands. In the saturation case, the induced shielding current reaches to the critical current of the strand. The constituent strands in parallel conductors usually need to be insulated and transposed for the sake of low ac loss and uniform current distribution. In the case that the strands are transposed at the optimum position, the interlinkage magnetic flux of the strands is cancelled out and the shielding current is not induced. But in the case that the transposition points deviate from optimum one, the shielding current is induced and the additional ac loss is occurred. We have already investigated the ac loss properties of 2-strand parallel conductors in the non-saturation case. However, if the field amplitude and/or the deviation in transposition are so large, the saturation condition is satisfied. We derived the expressions of the additional ac loss in the saturation case, and verified them by the experiment with the sample conductors composed of NbTi multifilamentary strands. As a result, the additional ac loss can be much reduced by transposition even in the saturation case.

**Keywords:** Parallel conductor, Oxide superconductor, Ac loss, Transposition, Shielding current, Saturation

### 1. Introduction

We introduced the parallel conductors composed of oxide superconductors as a new method of composing a large current capacity conductor. The constituent strands in parallel conductors usually need to be insulated and transposed for the sake of low ac loss and uniform current distribution. It is difficult to compose the parallel conductor with low-Tc superconducting strands, because the time constant of the current redistribution of the parallel conductor is so long that the local normal zone in a strand grows up and leads to the quench of the whole winding. But the specific heat of the oxide superconductor cooled with liquid nitrogen is hundreds times larger than one of the low-Tc superconductor, so we can assume that there is no quench in the oxide superconducting strand.

In the case that the strands are evenly transposed, the interlinkage magnetic flux of the strands is cancelled out and the shielding current is not induced. On the basis of this property, we built 500 kVA and 1000 kVA superconducting transformers cooled by liquid nitrogen with parallel conductors composed of Bi2223 superconducting multifilamen-

tary strands <sup>1),2)</sup>. The ac loss densities of the transformers are nearly on the same level of the constituent strands. This shows that the additional ac loss due to the formation of the parallel conductors are extremely small, because the transposition points of parallel conductors were decided by empirical knowledge to reduce the additional ac loss. But the transposition points may deviate from the optimum one in the design or the winding process. In this case the shielding current is induced and it produces the additional ac loss. So we have derived the theoretical expressions of additional ac loss due to the deviation of transposition on the 2-strand parallel conductor with one-point transposition exposed to spatially uniform magnetic field, and verified them by the experiment with the sample conductors composed of NbTi rectangular cross-sectional multifilamentary strands <sup>3),4)</sup>. In the study, we supposed that the shielding current does not reach to the critical current of the strands. However, when the field amplitude and/or the deviation in transposition are large, the shielding current reaches to the critical current.

In the non-saturation case that the shielding current is smaller than the critical current of the constituent strand, the interlinkage magnetic flux increases only through the decay of the induced shielding current. On the other hand, in the saturation case that the shielding current reaches up

\* Department of Electrical and Electronic Systems Engineering, Graduate Student

\*\* Department of Electrical and Electronic Systems Engineering

to the critical current, the magnetic flux penetrates into the inner region through the flux flow in the strands. The difference between both the cases is directly linked to the ac loss behavior.

In this paper, we discuss the ac loss properties in the saturation case and verify them by the experiment with the sample conductors composed of NbTi rectangular cross section multifilamentary strands.

## 2. Theory

For simple discussion, we defined the following situation. A 2-strand parallel conductor with one-point transposition is composed of rectangular cross-sectional superconducting multifilamentary strands. These strands have the dimensions of  $u$  in thickness and  $w$  in width and have many fine superconducting filaments that are symmetrically arranged in the cross section. **Figure 1** shows the schematic view of the transposed parallel conductor. The constituent strands are insulated and connected only at both the ends. The parallel conductor is exposed to uniform external magnetic field,  $B_e = \mu_0 H_e$ , which is parallel to the wide surface of the strands as shown in **Fig.1**. **Figure 2** shows the projective figure of the 2-strand parallel conductor. Here the transposition point deviates by  $\Delta\ell$  in length.  $L$  is the total conductor length and  $d_s$  is the distance between the centerlines of strands. The positive direction of the shielding current is shown by arrow in **Fig.2**. The shielding current,  $I$ , is induced so as to prevent the variation of the interlinkage magnetic flux. Here we assume that the shielding current is concentrated at the center in thickness of a strand and flows as uniform plane current with the same width as a strand as shown in **Fig.3**. The self magnetic field distribution due to the pair of plane current is also shown.

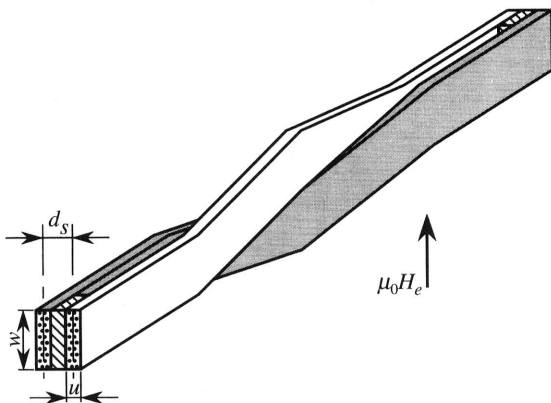


**Fig.1** Schematic view of a transposed 2-strand parallel conductor.

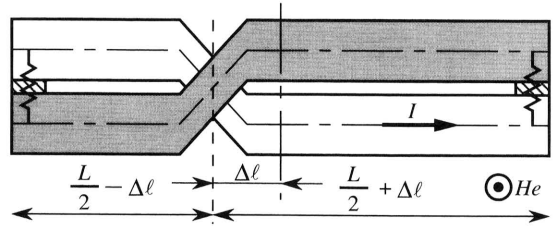


**Fig.2** Projective figure of a 2-strand parallel conductor in the direction of external magnetic field.

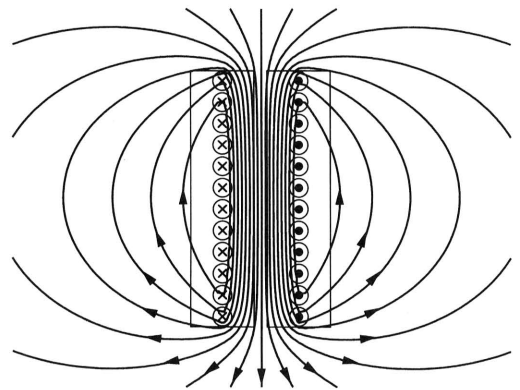


**Fig.3** Self magnetic field distribution due to a pair of uniform plane current in case of close contact.

The basic equation in the non-saturation case is expressed as <sup>4)</sup>

$$\left(\frac{2\Delta\ell}{L}\right) B_e - \tilde{B}_i = \tau \frac{d\tilde{B}_i}{dt} \quad (1)$$

$$\tilde{B}_i = \left(\frac{2\Delta\ell}{L}\right) B_e + \Delta B \quad (2)$$

$$\Delta B = \mu_0 k I = \mu_0 \frac{k'}{w} I \quad (3)$$

$$\tau = \mu_0 k \frac{d_s L}{2R} \quad (4)$$

where  $\tilde{B}_i$  is the average internal magnetic flux density and  $\tau$  is the decay time constant of the shielding current. Then we consider the situation that external magnetic field expressed as  $B_e = B_m \sin \omega t$  ( $\omega = 2\pi f$ ) is applied to the parallel conductor. Solving the basic equation, we obtain

$$I = -\frac{1}{k} \frac{\omega\tau}{\sqrt{1+(\omega\tau)^2}} \frac{B_m}{\mu_0} \left(\frac{2\Delta\ell}{L}\right) \sin(\omega t + \phi) \quad (5)$$

$$\phi = \tan^{-1}(1/\omega\tau) \quad (6)$$

Substituting  $I = I_c$  into Eq.(5), the saturation amplitude,  $B_s$ , is expressed as

$$B_s = \mu_0 k I_c \frac{\sqrt{1 + (\omega\tau)^2}}{\omega\tau} \left( \frac{L}{2\Delta\ell} \right) \quad (7)$$

Saturation condition is expressed as  $B_m > B_s$ .

In the saturation case, the amplitude of shielding current is kept as the critical current  $I_c$  even if the variation of interlinkage magnetic flux make it more larger. In this situation, Eq.(3) is expressed as

$$\Delta B_{max} = \mu_0 k I_c \quad (8)$$

Since the basic equation in the saturation case is expressed as

$$\left( \frac{2\Delta\ell}{L} \right) B_e - \tilde{B}_i = \mp \Delta B_{max} \quad (9)$$

where minus and plus sign of  $\Delta B_{max}$  correspond to the increasing and decreasing field process respectively.

Considering the situation that external magnetic field,  $B_e$ , begins to decrease from  $B_m$ , and the shielding current,  $I$ , begins to increase from  $-I_c$  to  $I_c$ . At the time that  $B_e = B_m(t = \pi/2\omega)$ , initial condition of  $\tilde{B}_i$  is expressed as

$$\tilde{B}_i = \left( \frac{2\Delta\ell}{L} \right) B_m - \Delta B_{max} \quad (10)$$

Substituting Eq.(10) to Eq.(2) and solving the basic equation, we obtain the expression of  $\tilde{B}_i$  and  $I$ . However these expressions are so complicated that we omit those here. Here we defined  $t_{sd}$  and  $t_{su}$  as the saturation time when  $I$  reaches to  $|I_c|$  in the decreasing- and increasing-field process. For the period,  $t_{sd} \leq t < 3\pi/2\omega$ ,  $I = I_c$  is satisfied and  $\tilde{B}_i$  is expressed by Eq.(9). In the increasing-field process, the expressions of  $I$  and  $\tilde{B}_i$  are obtained similarly.

The decay time constant,  $\tau$ , is proportional to the total conductor length as shown Eq.(4). In the practical situation, it is so long that the condition of  $\omega\tau \gg 1$  is satisfied.  $\tilde{B}_i$  and  $I$  are approximately expressed in this condition as

$$\tilde{B}_i = \begin{cases} \left( \frac{2\Delta\ell}{L} \right) B_m - \Delta B_{max} & : \text{(i)} \\ \left( \frac{2\Delta\ell}{L} \right) B_e + \Delta B_{max} & : \text{(ii)} \\ - \left( \frac{2\Delta\ell}{L} \right) B_m + \Delta B_{max} & : \text{(iii)} \\ \left( \frac{2\Delta\ell}{L} \right) B_e - \Delta B_{max} & : \text{(iv)} \end{cases} \quad (11)$$

$$I = \begin{cases} \frac{1}{k} \frac{B_m - B_e}{\mu_0} \left( \frac{2\Delta\ell}{L} \right) - I_c & : \text{(i)} \\ I_c & : \text{(ii)} \\ - \frac{1}{k} \frac{B_m + B_e}{\mu_0} \left( \frac{2\Delta\ell}{L} \right) + I_c & : \text{(iii)} \\ -I_c & : \text{(iv)} \end{cases} \quad (12)$$

where the symbols (i) to (iv) mean the periods as  $\pi/2\omega \leq t < t_{sd}$ ,  $t_{sd} \leq t < 3\pi/2\omega$ ,  $3\pi/2\omega \leq t < t_{su}$  and  $t_{su} \leq t < 5\pi/2\omega$  respectively.  $t_{sd}$  and  $t_{su}$  are also approximated as

$$t_{sd} = \frac{1}{\omega} \sin^{-1} \left\{ 1 - \frac{2\Delta B_{max}}{B_m} \left( \frac{L}{2\Delta\ell} \right) \right\} \quad (13)$$

$$t_{su} = \frac{1}{\omega} \sin^{-1} \left\{ -1 + \frac{2\Delta B_{max}}{B_m} \left( \frac{L}{2\Delta\ell} \right) \right\} \quad (14)$$

Substituting Eq.s (13) and (14) to  $B_e = B_m \sin \omega t$ , the saturation amplitude in the decreasing- and increasing-field process,  $B_{sd}$  and  $B_{su}$  are obtained as

$$B_{sd} = B_m - 2\Delta B_{max} \left( \frac{L}{2\Delta\ell} \right) \quad (15)$$

$$B_{su} = -B_m + 2\Delta B_{max} \left( \frac{L}{2\Delta\ell} \right) \quad (16)$$

The saturation amplitude,  $B_s$ , is also approximated as

$$B_s = \Delta B_{max} \left( \frac{L}{2\Delta\ell} \right) \quad (17)$$

Generally, the ac loss per unit volume of the strands and per one cycle is calculated by

$$W = \mu_0 \oint H_e dM \quad (18)$$

where  $M$  is the magnetization per unit volume of the strands and expressed as

$$M = \frac{I d_s}{2uw} \left( \frac{2\Delta\ell}{L} \right) \quad (19)$$

From Eq.s (2),(3) and (19), we obtain

$$dM = \frac{1}{\mu_0 k} \frac{d_s}{2uw} \left( \frac{2\Delta\ell}{L} \right) \left\{ d\tilde{B}_i - \left( \frac{2\Delta\ell}{L} \right) dB_e \right\} \quad (20)$$

Substituting Eq.(20) to Eq.(18), Eq.(18) leads to

$$\begin{aligned} W &= \frac{1}{k} \frac{d_s}{2uw} \left( \frac{2\Delta\ell}{L} \right) \oint H_e d\tilde{B}_i \\ &= -\frac{1}{\mu_0 k} \frac{d_s}{2uw} \left( \frac{2\Delta\ell}{L} \right) \oint \tilde{B}_i dB_e \\ &= -\frac{1}{\mu_0 k} \frac{d_s}{2uw} \left( \frac{2\Delta\ell}{L} \right) \left[ \int_{B_m}^{B_{sd}} \tilde{B}_i dB_e + \int_{B_{sd}}^{-B_m} \tilde{B}_i dB_e \right. \\ &\quad \left. + \int_{-B_m}^{B_{su}} \tilde{B}_i dB_e + \int_{B_{su}}^{B_m} \tilde{B}_i dB_e \right] \quad (21) \end{aligned}$$

By substituting Eq.(11) to Eq.(21), we obtain the expression of ac loss density per one cycle in the practical situation of  $\omega\tau \gg 1$  as

$$W = 4 \frac{I_c d_s}{2uw} \left( \frac{2\Delta\ell}{L} \right) (B_m - B_s) \quad (22)$$

### 3. Experiment

We verified the theoretical expressions by the experiment with the sample conductors composed of NbTi rectangular cross section multifilamentary strands. The characteristics of a strand is listed in **Table 1**. Two strands were cowound into one-layer solenoidal coils with various kinds of  $(2\Delta\ell/L)$ . The parameters of the sample coils are listed in **Table 2**. The contact resistance at a terminal,  $R$ , was nearly equal to  $3.8 \times 10^{-7} \Omega$ . Ac losses in the sample coils were measured by a pick-up coil method at 5 T dc bias field in liquid He by applying sinusoidal ac magnetic field with the amplitude ranged from 0.04 T to 0.4 T.

**Table-1** Characteristics of a NbTi superconducting multifilamentary wire

Superconductor	Nb-46.5Ti
Matrix	Cu-2Ni
Critical current, $I_c$ (A)	48.8 (at 5T)
CuNi/NbTi	4.762
Number of filaments	114
Twist pitch (mm)	8
Wire thickness, $u$ (mm)	0.196
Wire width, $w$ (mm)	1.097

The observed total ac losses are shown in **Fig.4** for the respective sample coils as compared with those in a strand. In any frequency, the ac loss in a strand agreed with the theoretical prediction calculated on the basis of Bean-London model with the measured  $I_c$  values. This shows that the observed ac loss in a strand is only the hysteresis loss in the superconducting filaments and the coupling current loss in a strand is negligible. The thick chain lines link the theoretical saturation amplitude,  $B_s$ , predicted from Eq.(7). The right areas of this lines correspond to the saturation cases. The thick solid lines link the ac loss in the parallel conductor calculated from Eq.(22). In any sample coils, frequency becomes higher i.e.  $\omega\tau$  becomes larger, the observed ac losses agreed with the theoretical lines. In the case of  $f = 2$  Hz, the condition  $\omega\tau \gg 1$  is satisfied. **Figure 5** shows the  $(2\Delta\ell/L)$  dependence of ac loss for  $B_m = 0.4$  T. We can see that the additional ac loss in the saturation case is proportional to the ratio of  $(2\Delta\ell/L)$  and the observed results agree with the theoretical expectation quantitatively.

**Figure 6** shows the magnetization curves at 1 Hz in the saturation case. We can see that the magnetization per unit volume of the strands,  $M$ , increase in proportion to  $(2\Delta\ell/L)$  as shown in Eq.(19). In addition, it is confirmed that the saturation amplitude,  $B_s$ , is inversely proportional to  $(2\Delta\ell/L)$  as expressed as Eq.(7). The magnetization, that is directly linked the ac loss, decreases in proportion to  $(2\Delta\ell/L)$  and the saturation amplitude becomes larger in inversely proportion to  $(2\Delta\ell/L)$ . These are remarkable properties and lead to low ac loss under the saturation condition.

### 4. Conclusion

We quantitatively investigated the ac loss properties of 2-strand parallel conductors composed of superconducting multifilamentary strands in the saturation case that the induced shielding current reach to the critical current of a strand. With using the basic equation in the non-saturation case, the basic equation and the theoretical expression of ac loss in the saturation case under the practical situation are derived. The results of certification experiments with using NbTi superconducting multifilamentary strands were explained by the theoretical expectation quantitatively. The ac loss density in parallel conductors can be reduced to the same level as a strand in the practical application stage even in the saturation case.

Table-2 Parameters of sample coils

	#A	#B	#C	#D
$(2\Delta\ell/L)$	0.2	0.4	0.6	1.0
Conductor length, $L$ (m)		2.6		
Inner diameter of a coil (mm)		42		
Height of a coil (mm)		50		
Number of turns		20		
Distance between the strands, $d_s$ (mm)		0.24		
Contact resistance at the end, $R(\times 10^{-7}\Omega)$	3.8	3.5	3.2	4.4
Theoretical decay time constant, $\tau$ (sec)	0.94	1.02	1.11	0.81

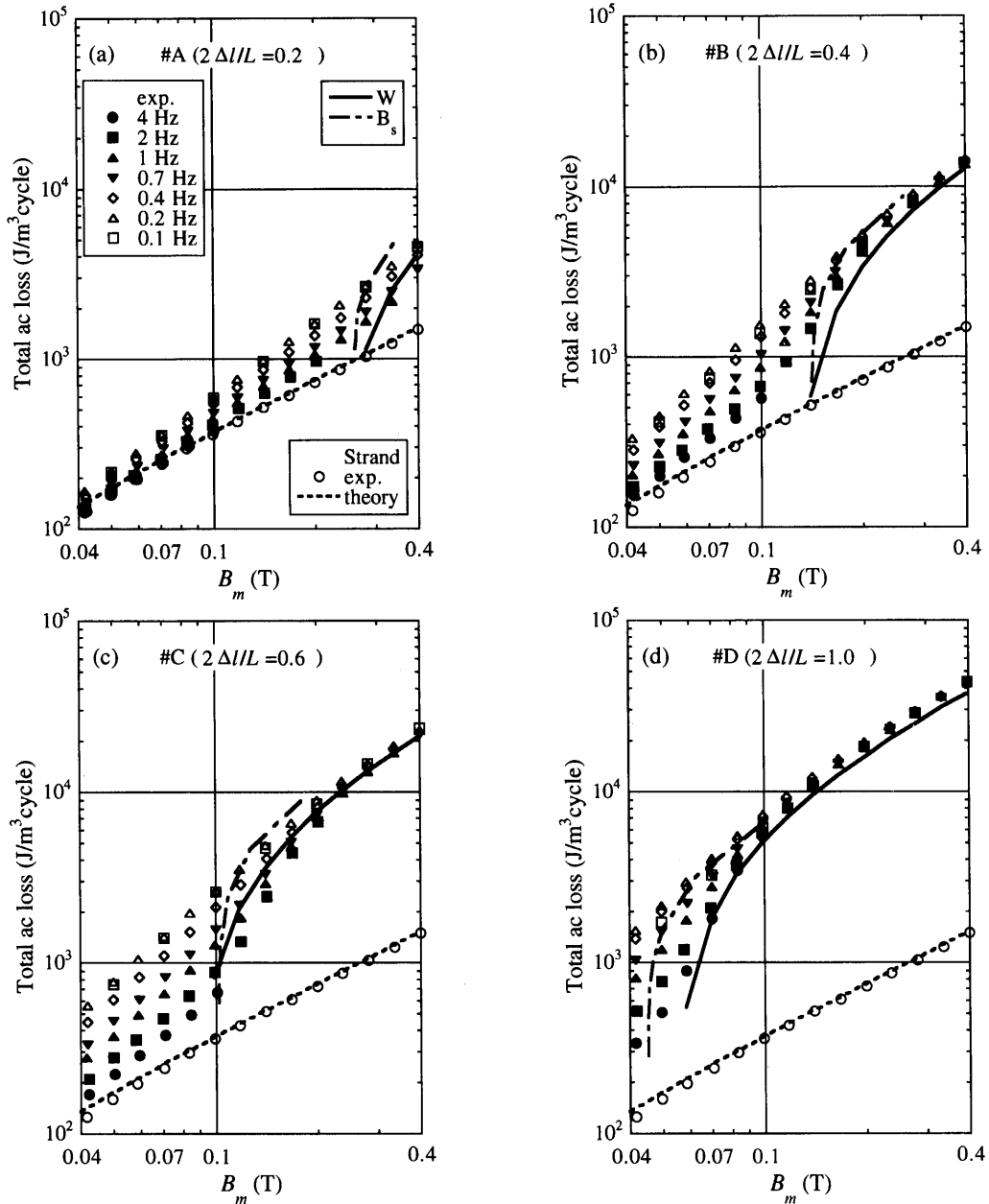
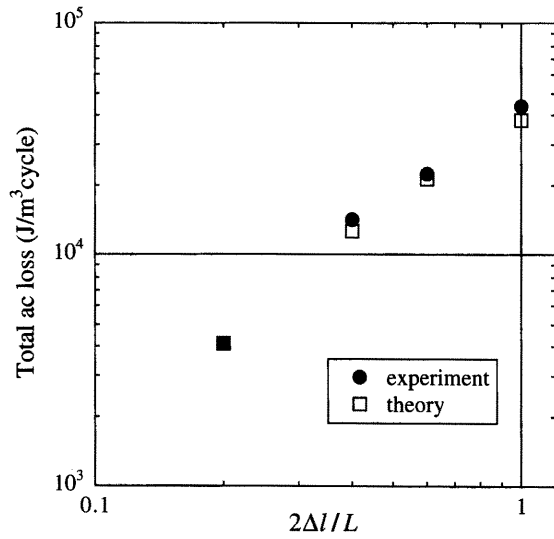
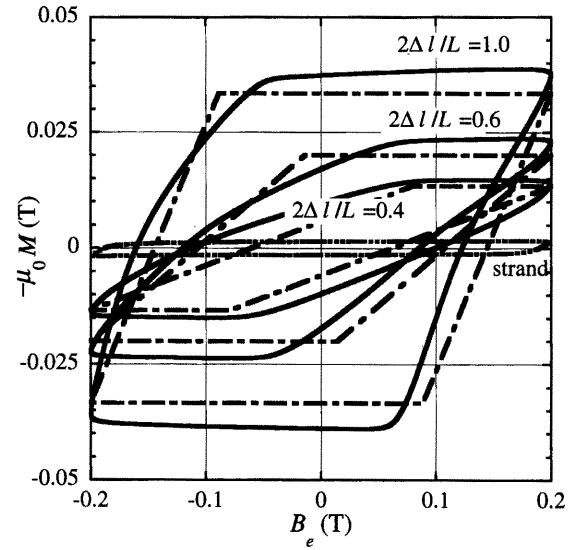


Fig.4 Field amplitude dependences of the total ac losses in (a) #A, (b) #B, (c) #C and (d) #D coils. The legend in (a) is in common in (b) to (d).



**Fig.5**  $(2\Delta l/L)$  dependence of the additional ac loss in the saturation case for  $B_m = 0.4$  T.



**Fig.6**  $(2\Delta l/L)$  dependence of the magnetization curves. The chained lines represent the theoretical predictions.

### References

- 1) Iwakuma, M.; Funaki, K.; Kajikawa, K.; Kanetaka H.; Hayashi, H.; Tsutsumi, K.; Tomioka, A.; Konno, M.; Nose, S. : *IEEE Trans. Appl. Supercond.* **9** (1999) 928-931
- 2) Funaki, K.; Iwakuma, M.; Kajikawa, K.; Hara, M.; Suehiro, J.; Ito, T.; Takata, Y.; Bohno, T.; Nose, S.; Konno, M.; Yagi, Y.; Maruyama, H.; Ogata, T.; Yoshida, S.; Ohashi, K.; Kimura, H.; Tsutsumi, K : *IEEE Trans. Appl. Supercond.* **11** (2001) 1578-1581
- 3) Tanaka, H.; Iwakuma, M.; Kajikawa, K.; Funaki, K.; Konno, M.; Nose, S.; Hayashi, K.; Sato, K. : *Advances in Supercond.* **12** (1999) 763-765
- 4) Iwakuma, M.; Tanaka, H.; Funaki, K. : "Ac loss properties of 2-strand parallel conductors composed of superconducting multifilamentary strands in non-saturation case" to be published *Superconductor Science and Technology*

